Chemical Physics Letters 458 (2008) 48–53

Contents lists available at ScienceDirect

Chemical Physics Letters

journal homepage: www.elsevier.com/locate/cplett

Noble gas–sulfur anions: A theoretical investigation of $FNgS^-$ (Ng = He, Ar, Kr, Xe)

Stefano Borocci, Nicoletta Bronzolino, Felice Grandinetti *

Dipartimento di Scienze Ambientali, Università della Tuscia, L.go dell' Università, s.n.c., 01100 Viterbo, Italy

ARTICLE INFO

Article history:
Received 6 February 2008
In final form 23 April 2008
Available online 29 April 2008

ABSTRACT

MP2, coupled-cluster, and multireference–CI calculations were performed to investigate the structure, stability, and properties of the noble gas anions $FNgS^-$ (Ng = He, Ar, Kr, Xe). Similar to the recently investigated $FNgO^-$ and $FNgBN^-$, these species reside into deep wells on the singlet surface, protected by sizable barriers with respect to $FS^- + Ng$ and $F^- + Ng + S(^3P)$. Their stability arises from the strong F^--stabilization of the elusive NgS. The lightest $FHeS^-$ and $FArS^-$ are also first predicted examples of helium–sulfur and argon–sulfur molecular species.

1. Introduction

Neutral and cationic species containing the noble gases (Ng) have been recently intensively investigated [1–3]. Various HNgX, including HArF [4], were observed in cold matrices [5], and other numerous XNgY have been also theoretically predicted [6–8] (X, Y = electronegative atoms or groups). Ng complexes of neutral and cationic transition metals were also observed [9,10]. Positive ions of the inert elements, including helium, are also continuously observed in the gas phase [11], and novel xenon cations are still isolated in the solid state [12]. The chemistry of the noble gas anions is instead less rich and variegated. Apart from few covalent xenon–oxygen and xenon–fluorine species [13,14], all the other inert elements usually form at the most weakly-bound anionic complexes. For example, the binding enthalpies of F^-–(Ng) (Ng = He, Ne, Ar, Kr) and O^-–(Ng) [16,17] range from 0.15 (Ng = He) to 4.1 kcal mol^{-1} (Ng = Kr) [15], and the Ng complexes of Cl^-, Br^-, I^-, and S^- are even less stable [15,18]. However, recent calculations by Hu and co-workers [19,20] and by us [21] revealed that the singlet $FNgO^-$ (Ng = He, Ar, Kr) and $FNgBN^-$ (Ng = He–Xe) are indeed strongly-bound metastable species, protected by sizable barriers from their exoergic dissociations. In particular, the meta-stability of $FNgO^-$ was rationalized as follows [19]. The singlet HeO ($^1\Sigma^+$) is not bound, while ArO and KrO are at least marginally stable with respect to Ng and O(^{1}D) [22]. However, at bond distances quite close to the energy minimum, they cross the purely repulsive triplet state ($^3\Pi$), and dissociate into the by far more stable Ng and O(^{3}P). In the presence of F^-, the singlet NgO resides in a deeper energy well. More importantly, the singlet $FNgO^-$ crosses the purely repulsive triplet state at Ng–O distances which are longer than the energy minimum by ca. 0.3 Å. This results in sizable crossing energies of ca. 7–15 kcal mol^{-1}. The spin-allowed decomposition of $FNgO^-$ into FO^- and Ng has also a high energy barrier. According to accurate calculations [23–25], the singlet ArS, KrS, and XeS (HeS and NeS are not bound) are even less stable than NgO. They are only weakly bound with respect to Ng and S(^{1}D), and separated by negligible crossing energies from the most stable Ng and S(^{3}P). We therefore decided to investigate whether the fluoride anion was still able to stabilize the singlet NgS with formation of $FNgS^-$ (Ng = He–Xe). Our calculations revealed that, with the only exception of $FNeS^-$, all these noble gas–sulfur anions reside into deep energy wells on the singlet surface, protected by sizable barriers from the dissociation into FS^- and Ng, and $F^- + Ng + S(^3P)$. We discuss here the structure, stability, and properties of these ions, and make also a brief comparison with the strictly related $FNgO^-$. The lightest $FHeS^-$ and $FArS^-$ are also first predicted examples of helium-sulfur and argon-sulfur molecular species.

2. Computational details

The calculations were performed with the Gaussian03 [26] and the Molpro 2000.1 programs [27] using the Dunning's correlation consistent double- and triple-zeta basis sets augmented with diffuse functions (He, O, F, Ne, S, Ar, and Kr atoms) [28] and the Stuttgart/Dresden (SDD) basis set with quasi-relativistic effective core potential (Xe atom) [29]. These basis sets, denoted here as aug-cc-pVDZ/SDD and aug-cc-pVTZ/SDD, were used to perform geometry optimizations and harmonic frequencies calculations at the second-order Møller–Plesset (MP2) [30] and at the coupled cluster level of theory, CCSD(T), [31,32] (frozen-core approximation). The geometry of $FHeS^-$ was also optimised, with the aug-cc-pVDZ basis set, at the multireference SCF level of theory, using a full-valence active space of 16 electrons distributed in 9 orbitals (CASSCF) [33], and at the multireference–configuration interaction (MR–CI) level of theory, using the internally contracted method implemented in Molpro [34,35]. The reference space consisted of all

* Corresponding author. Fax: +39 0761 357179.
E-mail address: fgrandi@unitus.it (F. Grandinetti).

0009-2614/$ - see front matter © 2008 Elsevier B.V. All rights reserved.
doi:10.1016/j.cplett.2008.04.098

the configurations arising from the CASSCF(16,9) wave function, and the CI procedure included the single and double excitations, and an estimate of higher-order excitations obtained by the multireference analogue of the Davidson correction [36]. The crossing energy for the decomposition of the singlet $FNgX^-$ into $F^- + Ng + X(^3P)$ (Ng = He, Ar, Kr, Xe; X = O, S) was estimated by locating, at the MP2/aug-cc-pVDZ/SDD level of theory, the minimum-energy point on the curve of intersection between the singlet and the (fully-repulsive) triplet $FNgX^-$ surface. To this end, the two surfaces were fully-scanned with respect to the bond distances (by steps of 0.05 Å) at fixed bond angles of 180°. The two obtained grids of points were interpolated by 3D plots and their zone of intersection of minimum energy was first estimated by graphical methods. The crossing structure was subsequently located by a further scan of this zone, stopped when the energy of the singlet and the triplet differed by less than 0.01 kcal mol^{-1}. For $FHeO^-$ and $FHeS^-$, the crossing structure was as well located at the CCSD(T)/aug-cc-pVDZ level of theory. The MP2/aug-cc-pVTZ/SDD atomic charges were calculated by natural bond orbital (NBO) analysis [37] of the wave function, and by the electrostatic potential-based method ChelpG [38], using the default value of point densities and the Bondi's van der Waals radius of Kr (2.02 Å) and Xe (2.16 Å) [39]. The chemical bonding analysis was based on the theory of atoms-in-molecules (AIM) [40] as implemented in the AIM 2000 [41]. We calculated the MP2/aug-cc-pVTZ/SDD charge density ρ, the Laplacian $\nabla^2\rho$, and the energy density H at the bond critical points (bcp), intended as the points on the attractor interaction lines where $\nabla\rho = 0$. Similar to the previously investigated HXeX (X = halogens) [42], the pseudopotential basis set used for Xe led to difficulties in the integration of the electron density of $FXeX^-$ (X = O, S), thus preventing the AIM analysis. The dissociation energies were corrected for the basis set superposition error (BSSE) by the method of Boys and Bernardi [43].

3. Results and discussion

The linear $FNgS^-$ shown in Fig. 1 were characterized as true minima on the singlet MP2 and CCSD(T) potential energy surfaces. The only exception is $FNeS^-$, whose attempted location invariably resulted, at any computational level, in the dissociated F^-, Ne, and $S(^1D)$. The computed bond distances, stabilities, and harmonic frequencies are listed in Tables 1–3. Unless stated otherwise, we will use for the discussion below the CCSD(T)/aug-cc-pVTZ/SDD estimates. The MP2/aug-cc-pVTZ/SDD total charges are reported in Table 4. As for the general validity of single-reference methods to describe the $FNgS^-$ anions, their CCSD T1 diagnostics [44] resulted invariably around the recommended threshold of 0.02. In addition, the CASSCF and MR–CI/aug-cc-pVDZ wave functions of the test-case $FHeS^-$ resulted by far dominated by the ground-state electronic configuration ($C_0 = 0.95$), and the computed bond distances were in good agreement with the MP2 and the CCSD(T) estimates (see Table 1).

The F^--induced stabilization of the singlet NgS ($^1\Sigma^+$) is clearly evident if one compares the structure and stability of these molecules with the data of Tables 1–3. The salient information is reported in Table 5. While HeS is unbound with respect to He and $S(^1D)$, the He–S distance of $FHeS^-$ is as short as 1.566 Å (1.585 Å at the MR–CI/aug-cc-pVDZ level of theory), and, for Ng = He, the ΔE(1a), defined here as the energy change of the dissociation

$$FNgS^- \rightarrow F^- + Ng + S(^1D) \quad (1a)$$

is nearly 8 kcal mol^{-1} (BSSE corrected value). The He–S stretching frequency is also 877 cm^{-1}. For the heaviest $FNgS^-$, ΔE(1a) regularly increases up to nearly 53 kcal mol^{-1}, while ΔE(1b), defined here as the energy change of the dissociation

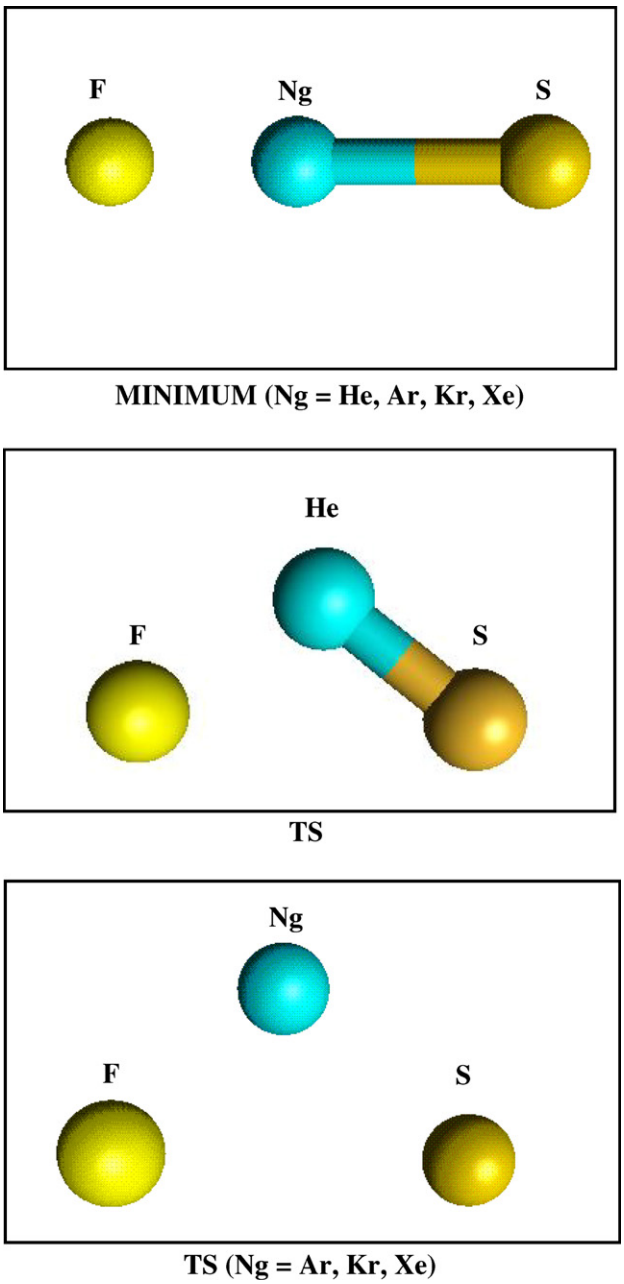

Fig. 1. Connectivities of the $FNgS^-$ energy minima and transition structures.

$$NgS \rightarrow Ng + S(^1D) \quad (1b)$$

is only 1.0 (Ng = Ar), 4.6 (Ng = Kr), and 12.3 kcal mol^{-1} (Ng = Xe), respectively. The Ng–S distances and harmonic frequencies of $FNgS^-$ are also invariably shorter and higher, respectively, than the corresponding NgS (see Table 5). We note also from Table 3 the relatively high IR intensities of both the Ng–S and F–Ng stretching frequencies and the regular increase of the F–Ng stretching mode passing from Ng = He to Ng = Xe. The F–Ng distances of $FNgS^-$ increase also from 1.793 Å for Ng = He to nearly identical values of ca. 2.3 Å for Ng = Ar, Kr, and Xe. Interestingly, at the CCSD(T)/aug-cc-pVTZ level of theory [19,21], the F-He distances of $FHeO^-$ and $FHeBN^-$ resulted as 1.626 and 1.725 Å, respectively, and the F–Ng distances of $FNgO^-$ (Ng = Ar, Kr) and $FNgBN^-$ (Ng = Ne, Ar, Kr, Xe) were invariably around 2.2–2.3 Å (similar to $FNeS^-$, $FNeO^-$ was not located as an energy minimum [19]). In addition, from Table 4, the F atom of any $FNgS^-$ has a large negative charge of ca.

Table 1
Optimized geometries (Å and °) of the $FNgS^-$ energy minima and transition structures (TS) (see Fig. 1)

Species	Method/basis set	Minimum ($C_{\infty v}$)		TS (C_s)		
		F–Ng	Ng–S	F–Ng	Ng–S	F–Ng–S
$FHeS^-$	MP2/aug-cc-pVDZ	1.852	1.563	2.148	1.853	104.7
	MP2/aug-cc-pVTZ	1.802	1.506	2.106	1.772	100.4
	CCSD(T)/aug-cc-pVDZ	1.845	1.647	2.219	2.070	118.0
	CCSD(T)/aug-cc-pVTZ	1.793	1.566	2.118	1.875	109.9
	CASSCF/aug-cc-pVDZ	1.956	1.602			
	MR-CI/aug-cc-pVDZ	1.879	1.585			
$FArS^-$	MP2/aug-cc-pVDZ	2.243	2.374	2.719	2.558	76.8
	MP2/aug-cc-pVTZ	2.170	2.314	2.645	2.445	71.6
	CCSD(T)/aug-cc-pVDZ	2.364	2.333	2.802	2.735	87.9
	CCSD(T)/aug-cc-pVTZ	2.318	2.246	2.702	2.525	79.3
$FKrS^-$	MP2/aug-cc-pVDZ	2.315	2.333	2.740	2.647	69.1
	MP2/aug-cc-pVTZ	2.277	2.274	2.660	2.543	65.0
	CCSD(T)/aug-cc-pVDZ	2.336	2.411	2.800	2.744	76.0
	CCSD(T)/aug-cc-pVTZ	2.300	2.333	2.713	2.590	69.6
$FXeS^-$	MP2/aug-cc-pVDZ/SDD	2.328	2.445	2.726	2.703	60.7
	MP2/aug-cc-pVTZ/SDD	2.312	2.423	2.672	2.678	59.1
	CCSD(T)/aug-cc-pVDZ/SDD	2.351	2.494	2.736	2.777	64.4
	CCSD(T)/aug-cc-pVTZ/SDD	2.337	2.466	2.703	2.729	62.2

Table 2
Dissociation energies at 0 K (kcal mol^{-1}) of the $FNgS^-$ anions (reference species) calculated with the aug-cc-pVTZ/SDD basis set

Species	Method	$F^- + NgS$[a]	$F^- + Ng + S(^1D)$	$F + Ng + S^-$	$F^- + Ng + S(^3P)$	$FS^- + Ng$	Barrier[b]	Crossing[c]
$FHeS^-$	MP2		15.7	13.3	−26.0	−78.2	6.5	1.7
	CCSD(T)		9.6 (8.1[d])	10.4	−21.1	−74.7	4.8	0.7[e]
$FArS^-$	MP2	23.8	31.8	29.4	−9.9	−62.1	17.5	1.3
	CCSD(T)	21.9	23.4 (21.8[d])	24.2	−7.3	−60.9	14.3	
$FKrS^-$	MP2	33.2	48.3	45.9	6.6	−45.6	28.6	5.9
	CCSD(T)	32.1	38.3 (35.1[d])	39.1	7.6	−46.0	24.4	
$FXeS^-$	MP2	43.1	67.8	65.4	26.1	−26.0	41.5	16.4
	CCSD(T)	42.0	56.4 (52.8[d])	57.2	25.7	−27.9	36.1	

[a] HeS is not bound.
[b] Energy barrier at 0 K of the reaction $FNgS^- \rightarrow FS^- + Ng$.
[c] MP2/aug-cc-pVDZ/SDD crossing energy of the reaction $FNgS^- \rightarrow F^- + Ng + S(^3P)$.
[d] BSSE corrected value.
[e] CCSD(T)/aug-cc-pVDZ/SDD crossing energy of the reaction $FNgS^- \rightarrow F^- + Ng + S(^3P)$.

Table 3
Harmonic vibrational frequencies (cm^{-1}) of the linear $FNgS^-$

Species	Method/basis set	Assignment		
		ν(F–Ng)	ν(Ng–S)	δ(F–Ng–S)[a]
$FHeS^-$	MP2/aug-cc-pVDZ	179 (109)	942 (62)	236 (8)
	MP2/aug-cc-pVTZ	202 (107)	1029 (91)	259 (8)
	CCSD(T)/aug-cc-pVDZ	164	774	225
	CCSD(T)/aug-cc-pVTZ	192	877	241
$FArS^-$	MP2/aug-cc-pVDZ	201 (184)	379 (32)	106 (23)
	MP2/aug-cc-pVTZ	220 (192)	415 (39)	115 (23)
	CCSD(T)/aug-cc-pVDZ	197	316	103
	CCSD(T)/aug-cc-pVTZ	217	350	110
$FKrS^-$	MP2/aug-cc-pVDZ	243 (261)	346 (78)	116 (27)
	MP2/aug-cc-pVTZ	266 (259)	374 (75)	121 (26)
	CCSD(T)/aug-cc-pVDZ	233	299	108
	CCSD(T)/aug-cc-pVTZ	257	329	111
$FXeS^-$	MP2/aug-cc-pVDZ	300 (236)	344 (120)	120 (27)
	MP2/aug-cc-pVTZ	304 (250)	356 (106)	122 (26)
	CCSD(T)/aug-cc-pVDZ/SDD	277	317	113
	CCSD(T)/aug-cc-pVTZ/SDD	285	327	115

IR intensities (km mol^{-1}) are given in parentheses.
[a] Doubly-degenerate bending motion.

Table 4
MP2/aug-cc-pVTZ/SDD atomic charges (e) of the $FNgS^-$ energy minima and transition structures (TS) (see Fig. 1)

Species	Method	Minimum			TS		
		F	Ng	S	F	Ng	S
$FHeS^-$	NBO	−0.944	0.246	−0.302	−0.973	0.113	−0.140
	ChelpG	−0.899	0.317	−0.418	−0.887	0.139	−0.252
$FArS^-$	NBO	−0.920	0.385	−0.465	−0.970	0.164	−0.194
	ChelpG	−0.843	0.369	−0.526	−0.829	0.086	−0.257
$FKrS^-$	NBO	−0.873	0.521	−0.648	−0.946	0.218	−0.272
	ChelpG	−0.775	0.426	−0.651	−0.772	0.081	−0.309
$FXeS^-$	NBO	−0.848	0.700	−0.852	−0.912	0.299	−0.387
	ChelpG	−0.698	0.431	−0.733	−0.690	0.056	−0.366
ArS	NBO		0.212	−0.212			
	ChelpG		0.195	−0.195			
KrS	NBO		0.339	−0.339			
	ChelpG		0.266	−0.266			
XeS	NBO		0.511	−0.511			
	ChelpG		0.330	−0.330			

−0.8/−0.9 e (only for $FXeS^-$ the ChelpG predicts a slightly more pronounced charge transfer from F to S), and the noble gas–sulfur charge separation of any $FNgS^-$ (Ng = Ar, Kr, Xe) is invariably larger than the corresponding NgS. We found also that, at the bcp of the F–Ng bond of $FHeS^-$, $FArS^-$, and $FKrS^-$, ρ is low (between ca. 0.3 and 0.4 e $Å^{-3}$), $\nabla^2\rho$ is positive (between ca. 4 and 6 e $Å^{-5}$), and H is

Table 5
Bond distances (Å), harmonic vibrational frequencies (cm^{-1}), and dissociation energies (kcal mol^{-1}) of the singlet NgS($^1\Sigma^+$) and $FNgS^-$ computed at the CCSD(T)/aug-cc-pVTZ level of theory (Ng = He, Ar, Kr, Xe)

Species	R(F–Ng)	R(Ng–S)	ν(F–Ng)[b]	ν(Ng–S)[b]	δ(F–Ng–S)[b,c]	ΔE[d]
$FHeS^-$[a]	1.793	1.566	192 (107)	877 (91)	241 (8)	9.6 (8.1)
$FArS^-$	2.318	2.246	217 (192)	350 (39)	110 (23)	23.4 (21.8)
ArS		2.615		78 (20)		1.5 (1.0)
$FKrS^-$	2.300	2.333	257 (259)	329 (75)	111 (26)	38.3 (35.1)
KrS		2.446		196 (12)		6.2 (4.6)
$FXeS^-$	2.337	2.466	285 (250)	327 (106)	115 (26)	56.4 (52.8)
XeS		2.489		259 (3)		14.4 (12.3)

[a] HeS is not bound.
[b] The MP2/aug-cc-pVTZ/SDD IR intensity (km mol^{-1}) is given in parenthesis.
[c] Doubly-degenerate bending motion.
[d] Energy change at 0 K of the reaction $FNgS^- \rightarrow F^- + Ng + S(^1D)$ or $NgS \rightarrow Ng + S(^1D)$. BSSE corrected value is given in parenthesis.

vanishingly small. Overall, similar to the $FNgO^-$ and $FNgBN^-$, the $FNgS^-$ must be structurally viewed as F^-–(NgS) ion–dipole complexes.

Apart from reaction (1a), the overall stability of the singlet $FNgS^-$ depends on the energetics and the activation barriers of the dissociations

$$FNgS^- \rightarrow F + Ng + S^- \quad (2)$$

$$FNgS^- \rightarrow F^- + Ng + S(^3P) \quad (3)$$

$$FNgS^- \rightarrow FS^- + Ng \quad (4)$$

For any Ng, the ΔE of (2) is definitely positive. For Ng = Kr and Xe, the spin-forbidden reaction (3) is endothermic by 7.6 and 25.8 kcal mol^{-1}, respectively (the MP2/aug-cc-pVDZ/SDD energy changes are −4.4 and 18.1 kcal mol^{-1}, respectively), and the corresponding MP2/aug-cc-pVDZ/SDD crossing energies are 5.9 and 16.4 kcal mol^{-1}, respectively. For Ng = He and Ar, reaction (3) is exothermic by 21.1 and 7.3 kcal mol^{-1}, respectively, but the crossing energies are still positive and computed as 1.7 (Ng = He) and 1.3 kcal mol^{-1} (Ng = Ar). (At the CCSD(T)/aug-cc-pVDZ level of theory, the crossing energy of $FHeS^-$ is still positive and computed as 0.7 kcal mol^{-1}). At any crossing structure, the Ng–S bond distance resulted invariably longer than the corresponding energy minimum, and the predicted differences of 0.182 Å (Ng = He), 0.001 Å (Ng = Ar), 0.267 Å (Ng = Kr), and 0.442 Å (Ng = Xe) parallel the trend of the crossing energies. Reaction (4) is invariably largely exothermic. However, for any Ng, the involved activation barrier is positive and regularly increases from ca. 5 kcal mol^{-1} for Ng = He to ca. 36 kcal mol^{-1} for Ng = Xe. The process occurs through the bent transition structures (TS) shown in Fig. 1. Their relevant properties are listed in Tables 1 and 4 (similar to the energy minima, their CCSD T1 diagnostics resulted invariably around the threshold of 0.02). Passing from the minimum to the TS, the F–Ng bond elongates by ca. 0.5 Å, and the F–Ng–S bond angle reduces by ca. 60° for $FHeS^-$, and by more than 100–110° for the heaviest congeners. The single imaginary frequency detected for the transition state is invariably associated with the F–Ng–S bending motion and computed in particular at the CCSD(T)/aug-cc-pVTZ/SDD level of theory as 365i (Ng = He), 169i (Ng = Ar), 246i (Ng = Kr), and 330i cm^{-1} (Ng = Xe). From Table 4, the F atom of any TS retains a large negative charge and the charge separation between Ng and S slightly reduces with respect to the energy minimum. This suggests that reaction (4) occurs by a fluoride anion which 'walks around' the NgS moiety.

Quantitative criteria have been recently proposed for the metastability of the noble gas molecules XNgY (X and Y other than H)

Table 6
Properties of the linear $FNgX^-$ (X = O, S)

	$FHeO^-$	$FHeS^-$	$FArO^-$	$FArS^-$	$FKrO^-$	$FKrS^-$	$FXeO^-$	$FXeS^-$
R(F–Ng)[a]	1.626[b]	1.793	2.241[b]	2.318	2.259[b]	2.300	2.321	2.337
R(Ng–X)[a]	1.110[b]	1.566	1.781[b]	2.246	1.854[b]	2.333	1.967	2.466
ν(F–Ng)[c]	331 (116)[b]	192 (107)	275 (69)[b]	217 (192)	294 (234)[b]	257 (259)	306 (230)	285 (250)
ν(Ng–X)[c]	1273 (183)[b]	877 (91)	535 (192)[b]	350 (39)	539 (130)[b]	329 (75)	563 (178)	327 (106)
δ(F–Ng–X)[c]	449 (35)[b]	241 (8)	175 (37)[b]	110 (23)	170 (40)[b]	111 (26)	164 (41)	115 (26)
q(F)[d]	−0.910	−0.944	−0.897	−0.920	−0.855	−0.873	−0.842	−0.848
q(Ng)[d]	0.571	0.246	0.727	0.385	0.862	0.521	1.027	0.700
q(X)[d]	−0.662	−0.302	−0.832	−0.465	−1.010	−0.648	−1.187	−0.852
ΔE (F^- + NgX)[e]			29.7[b]	21.9	37.4[b]	32.1	43.3	42.0
ΔE [F^- + Ng + X(^{1}D)][e]	19.2[b]	9.7	37.1[b]	23.4	58.1[b]	38.3	80.3	56.4
ΔE (F + Ng + X^-)[e]	14.1[b]	10.4	32.0[b]	24.2	52.9[b]	39.1	75.1	57.2
ΔE [F^- + Ng + X(^{3}P)][e]	−31.6[b]	−21.1	−13.7[b]	−7.3	7.3[b]	7.6	29.5	25.8
ΔE (FX^- + Ng)[e]	−55.3[b]	−74.7	−37.4[b]	-60.9	−16.4[b]	−46.0	6.9	−27.9
Barrier[f]	14.4[b]	4.8	30.6[b]	14.3	49.0[g]	24.4	66.1	36.1
Crossing[h]	11.4 (4.9[i])	1.7 (0.7[i])	7.6	1.3	17.6	5.9	32.2	16.4

[a] CCSD(T)/aug-cc-pVTZ/SDD bond distance (Å).
[b] Taken from Ref. [19].
[c] CCSD(T)/aug-cc-pVTZ/SDD harmonic frequency (cm^{-1}). The MP2/aug-cc-pVTZ/SDD IR intensity (km mol^{-1}) is given in parenthesis.
[d] MP2/aug-cc-pVTZ/SDD NBO total charge (e).
[e] CCSD(T)/aug-cc-pVTZ/SDD energy change at 0 K (kcal mol^{-1}). $FNgX^-$ is the reference species.
[f] CCSD(T)/aug-cc-pVTZ/SDD energy barrier at 0 K of the reaction $FNgX^- \rightarrow FX^- + Ng$.
[g] Single-point energy at CCSD(T)/aug-cc-pVDZ structure with no ZPE (taken from Ref. [19]).
[h] MP2/aug-cc-pVDZ/SDD crossing energy of the reaction $FNgX^- \rightarrow F^- + Ng + X(^3P)$.
[i] CCSD(T)/aug-cc-pVDZ crossing energy of the reaction $FHeX^- \rightarrow F^- + He + X(^3P)$ (X = O or S).

[45]. In particular, in order to have a half-life of ca. 100 s in the gas phase at 100, 200, and 300 K, the dissociation into X + Ng + Y must have a barrier of 9, 17, and 25 kcal mol^{-1}, respectively, and the dissociation into Ng + XY must have barriers of 6, 13, and 21 kcal mol^{-1}, respectively. Therefore, from Table 2, $FKrS^-$ and $FXeS^-$ could be metastable on the singlet surface up to ca. 100 and 200 K, respectively. The lower decomposition barriers of $FHeS^-$ and $FArS^-$ are probably still large enough to suggest their conceivable existence at the low temperatures of cold matrices.

Table 6 compares the salient features of the $FNgX^-$ anions (X = O, S). For any Ng, the sulfur-containing structure is in general less compact and more weakly bound. For example, the Ng–S bond distances are invariably longer than the corresponding Ng–O, the harmonic frequencies are invariably lower, and the dissociations into $F^- + Ng + X(^1D)$ and $F + Ng + X^-$ are invariably less endothermic for X = S. The activation energies for the decompositions into $F^- + Ng + X(^3P)$ and $FX^- + Ng$ are also comparatively lower. Both $FNgO^-$ and $FNgS^-$ must be viewed as F^-–(NgX) ion–dipole complexes. This is suggested by the total charges of the F atoms, and is confirmed, at least for Ng = He, Ar, and Kr, by the contour lines diagrams, plotted in Fig. 2, of the $\nabla^2\rho$. The lines around the F atoms are in particular nearly spheric, with only slight progressively increasing deformations from $FHeX^-$ to $FKrX^-$. As for the Ng–O and Ng–S interaction, the bond between noble gases and closed shell fragments, whether ionic or covalent or both, raises in general animated debate in the literature [46,47]. Fig. 2 suggests that, at least for $FHeX^-$, $FArX^-$, and $FKrX^-$, the Ng–X interaction is essentially ionic, with a decreasing polar character from the oxygen to the sulfur congener. The contour lines of the $\nabla^2\rho$ around the Ng atoms are in fact nearly spheric, and only show deformations more pronounced for the oxygen species. From Table 6, the Ng–X charge separation is also more pronounced for X = O.

In conclusion, our calculations support the theoretical prediction of $FNgS^-$, a novel group of noble gas anions strictly related to $FNgO^-$ [19] and $FNgBN^-$ [21]. The only noble gas–sulfur compound observed to date is the neutral HXeSH prepared in cold matrices and identified by IR spectroscopy [48]. Interestingly, the CCSD(T) predicted stability with respect to H + Xe + SH, nearly 9 kcal mol^{-1}, is even lower than our predicted decomposition barriers of $FXeS^-$. The Xe-S bond distance and stretching frequency of HXeSH (2.775 Å and 218 cm^{-1}) are also longer and lower, respectively, than $FXeS^-$. The neutral HKrSH resulted metastable at the MP2 level of theory [49], but this prediction was questioned by subsequent CCSD(T) calculations [50]. No other noble gas–sulfur compounds have been to date observed or predicted. Therefore, $FHeS^-$ and $FArS^-$ are first examples of helium-sulfur and argon–sulfur molecular species; their predicted properties suggest however that they are more likely to be unstable than metastable.

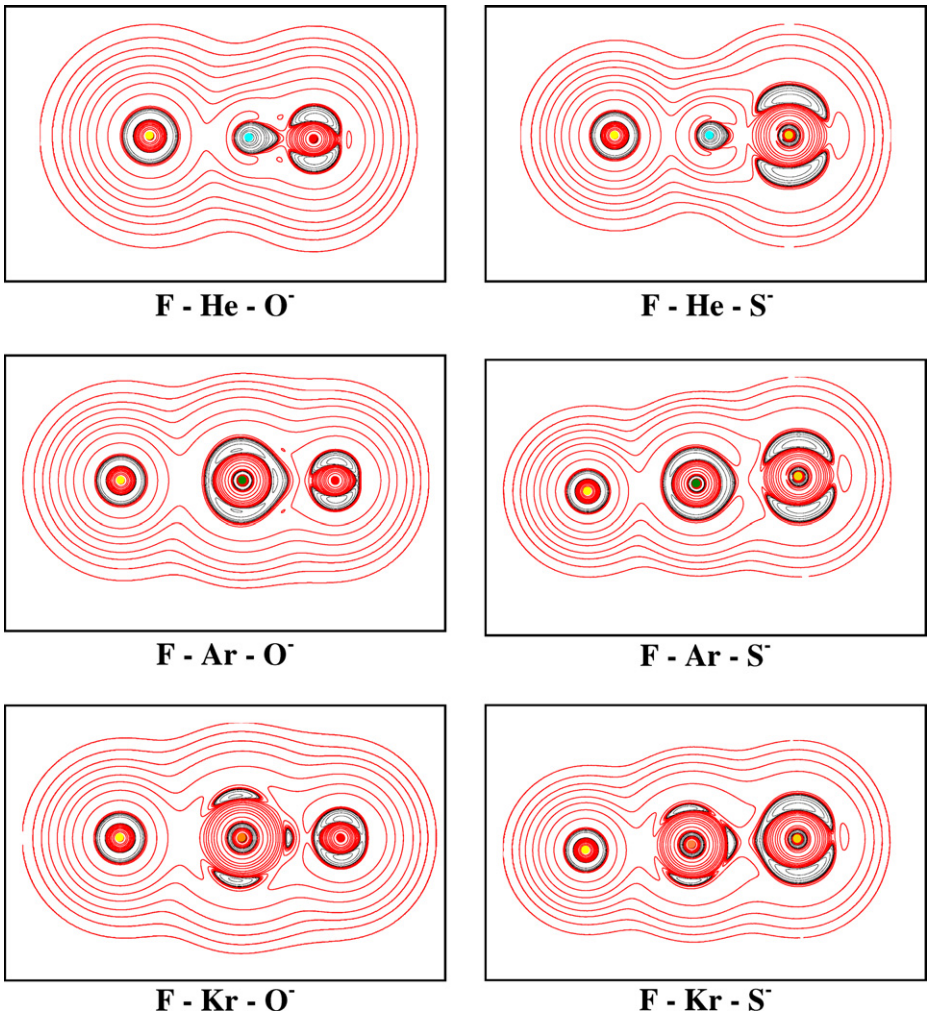

Fig. 2. Contour lines diagrams of the MP2/aug-cc-pVTZ/SDD Laplacian of the electronic charge density $-\nabla^2\rho(\mathbf{r})$ of $FNgO^-$ and $FNgS^-$ (Ng = He, Ar, Kr). Red and black lines are in regions of charge depletion ($-\nabla^2\rho(\mathbf{r}) < 0$) and charge concentration ($-\nabla^2\rho(\mathbf{r}) > 0$), respectively.

Acknowledgements

We thank the Italian Ministero dell' Università e della Ricerca (MiUR) for financial support.

References

[1] W. Grochala, Chem. Soc. Rev. 36 (2007) 1632.
[2] R.B. Gerber, Annu. Rev. Phys. Chem. 55 (2004) 55.
[3] S.A.C. McDowell, Curr. Org. Chem. 10 (2006) 791.
[4] L. Khriachtchev, M. Pettersson, N. Runeberg, J. Lundell, M. Räsänen, Nature 406 (2000) 874.
[5] A. Lignell, L. Khriachtchev, J. Lundell, H. Tanskanen, M. Räsänen, J. Chem. Phys. 125 (2006) 184514.
[6] T. Jayasekharan, T.K. Ghanty, J. Chem. Phys. 125 (2006) 234106.
[7] L. Sheng, R.B. Gerber, J. Chem. Phys. 126 (2007) 021108.
[8] S. Yockel, E. Gawlik, A.K. Wilson, J. Phys. Chem. A 111 (2007) 11261.
[9] S. Seidel, K. Seppelt, Science 290 (2000) 117.
[10] J. Li, B.E. Bursten, B. Liang, L. Andrews, Science 295 (2002) 2242.
[11] F. Grandinetti, Int. J. Mass Spectrom. 237 (2004) 243.
[12] S. Seidel, K. Seppelt, C. van Wuellen, X.Y. Sun, Angew. Chem. Int. Ed. 46 (2007) 6717.
[13] M.A.M. Forgeron, R.E. Wasylishen, M. Gerken, G.J. Schrobilgen, Inorg. Chem. 46 (2007) 3585.
[14] I.H. Krouse, C. Hao, C.E. Check, K.C. Lobring, L.S. Sunderlin, P.G. Wenthold, J. Am. Chem. Soc. 129 (2007) 846.
[15] A. Wada, A. Kikkawa, T. Sugiyama, K. Hiraoka, Int. J. Mass Spectrom. 267 (2007) 284.
[16] L.A. Viehland, R. Webb, E.P.F. Lee, T.G. Wright, J. Chem. Phys. 122 (2005) 114302.
[17] A.A. Buchachenko, M.M. Szczęśniak, J. Klos, G. Chalasiński, J. Chem. Phys. 117 (2002) 2629.
[18] T.G. Wright, L.A. Viehland, Chem. Phys. Lett. 420 (2006) 24.
[19] T.-H. Li, C.-H. Mou, H.-R. Chen, W.-P. Hu, J. Am. Chem. Soc. 127 (2005) 9241.
[20] Y.-L. Liu, Y.-H. Chang, T.-H. Li, H.-R. Chen, W.-P. Hu, Chem. Phys. Lett. 439 (2007) 14.
[21] P. Antoniotti, S. Borocci, N. Bronzolino, P. Cecchi, F. Grandinetti, J. Phys. Chem. A 111 (2007) 10144.
[22] T.H. Dunning Jr., P.J. Hay, J. Chem. Phys. 66 (1977) 3767.
[23] M. Yamanishi, K. Hirao, K. Yamashita, J. Chem. Phys. 108 (1998) 1514.
[24] A.V. Nemukhin, B.L. Grigorenko, A.A. Granovsky, Chem. Phys. Lett. 301 (1999) 287.
[25] T. Kiljunen, J. Eloranta, H. Kunttu, L. Khriachtchev, M. Pettersson, M. Räsänen, J. Chem. Phys. 112 (2000) 7475.
[26] M.J. Frish, et al., Gaussian 03, Revision C.02, Gaussian, Inc., Wallingford, CT, 2004.
[27] Molpro is a package of ab initio programs written by H.-J. Werner and P.J. Knowles, with contributions from R.D. Amos, A. Bernhadsson, A. Berning, P. Celani, D.L. Cooper, M.J.O. Deegan, A.J. Dobbyn, F. Eckert, C. Hampel, G. Hetzer, T. Korona, R. Lindh, A.W. Lloyd, S.J. McNicholas, F.R. Manby, W. Meyer, M.E. Mura, A. Nicklass, P. Palmieri, R. Pitzer, G. Rauhut, M. Schatz, H. Stoll, A.J. Stone, R. Tarroni, T. Thorsteinsson.
[28] R.A. Kendall, T.H. Dunning Jr., R.J. Harrison, J. Chem. Phys. 96 (1992) 6796.
[29] A. Nicklass, M. Dolg, H. Stoll, H. Preuss, J. Chem. Phys. 102 (1995) 8942. Denoted as ECP46MWB.
[30] C. Møller, M.S. Plesset, Phys. Rev. 46 (1934) 618.
[31] K. Raghavachari, G.W. Trucks, J.A. Pople, M. Head-Gordon, Chem. Phys. Lett. 157 (1989) 479.
[32] C. Hampel, K. Peterson, H.-J. Werner, Chem. Phys. Lett. 190 (1992) 1.
[33] H.-J. Werner, P.J. Knowles, J. Chem. Phys. 82 (1985) 5053.
[34] H.-J. Werner, P.J. Knowles, J. Chem. Phys. 89 (1988) 5803.
[35] P.J. Knowles, H.-J. Werner, Chem. Phys. Lett. 145 (1988) 514.
[36] S.R. Langhoff, D.E. Davidson, Int. J. Quantum Chem. 8 (1974) 61.
[37] E.D. Glendening, A.E. Reed, J.E. Carpenter, F. Weinhold, NBO, Version 3.1.
[38] C.M. Breneman, K.B. Wiberg, J. Comput. Chem. 11 (1990) 361.
[39] A. Bondi, J. Phys. Chem. 68 (1964) 441.
[40] R.F.W. Bader, Atoms in Molecules: a Quantum Theory, Oxford University Press, Oxford, 1990.
[41] Aim2000, designed by F. Biegler-König, University of Applied Sciences, Bielefeld, Germany, <http://www.AIM2000.de>.
[42] J. Panek, Z. Latajka, J. Lundell, Phys. Chem. Chem. Phys. 4 (2002) 2504.
[43] S. Boys, F. Bernardi, Mol. Phys. 19 (1970) 553.
[44] T.J. Lee, P.R. Taylor, Int. J. Quantum Chem. Quantum Chem. Symp. 23 (1989) 199.
[45] T.-H. Li, Y.-L. Liu, R.-J. Lin, T.-Y. Yeh, W.-P. Hu, Chem. Phys. Lett. 434 (2007) 38.
[46] P. Pyykkö, J. Am. Chem. Soc. 117 (1995) 2067.
[47] J.P. Read, A.D. Buckingham, J. Am. Chem. Soc. 119 (1997) 9010.
[48] M. Pettersson, J. Lundell, L. Khriachtchev, E. Isoniemi, M. Räsänen, J. Am. Chem. Soc. 120 (1998) 7979.
[49] S.A.C. McDowell, Chem. Phys. Lett. 372 (2003) 553.
[50] J. Lundell, L. Khriachtchev, M. Pettersson, M. Räsänen, Chem. Phys. Lett. 388 (2004) 228.